

Elastic scattering of ^{10}Be on ^{208}Pb near the Coulomb barrierJ. J. Kolata,¹ E. F. Aguilera,² F. D. Becchetti,³ Yu Chen,³ P. A. DeYoung,⁴ H. García-Martínez,² J. D. Hinnefeld,⁵ J. H. Lupton,³ E. Martínez-Quiroz,² and G. Peaslee⁶¹Physics Department, University of Notre Dame, Notre Dame, Indiana 46556-5670, USA²Departamento del Acelerador, Instituto Nacional de Investigaciones Nucleares, Apartado Postal 18-1027, C.P. 11801, D.F. Mexico³Physics Department, University of Michigan, Ann Arbor, Michigan 48109-1120, USA⁴Physics Department, Hope College, Holland, Michigan 49422-9000, USA⁵Physics Department, Indiana University South Bend, South Bend, Indiana 46634-7111, USA⁶Chemistry Department, Hope College, Holland, Michigan 49422-9000, USA

(Received 26 February 2003; published 16 April 2004)

The elastic scattering of ^{10}Be on ^{208}Pb has been measured over a range of energies near the nominal Coulomb barrier. An excitation function for the total reaction cross section is obtained from the elastic-scattering angular distributions and compared with existing fusion data. Comparisons are also made with existing fusion, transfer/breakup, and elastic data for ^9Be incident on ^{209}Bi . A strong enhancement in the sub-barrier total reaction cross section for $^9\text{Be}+^{209}\text{Bi}$ relative to $^{10}\text{Be}+^{208}\text{Pb}$ is demonstrated.

DOI: 10.1103/PhysRevC.69.047601

PACS number(s): 25.60.Bx, 25.60.Dz, 27.20.+n

Reaction cross sections for a number of weakly bound light nuclei incident on high- Z targets have recently been reported at energies near the Coulomb barrier [1–6]. The focus in these experiments was on the transfer/breakup mode. This mode is exceptionally strong in the $^6\text{He}+^{209}\text{Bi}$ reaction and actually exceeds the fusion yield at the barrier, saturating essentially all of the sub-barrier total reaction cross section [1]. Similar but less extreme behavior of the transfer/breakup yield was subsequently observed for stable, weakly bound light nuclei in reactions such as $^9\text{Be}+^{209}\text{Bi}$ [4] and $^{6,7}\text{Li}+^{208}\text{Pb}$ [2,3,6], and also for $^8\text{Li}+^{208}\text{Pb}$ [5].

Elastic-scattering data near the barrier have also been obtained [5,7–9] for all the systems mentioned above. These data can be analyzed to extract excitation functions for the total reaction cross section. It is then interesting to compare the results with those for a more tightly bound projectile such as ^{10}Be , which has a breakup threshold of 6.8 MeV. Reaction cross-section data for this nucleus are particularly valuable since they serve as an ideal base line for comparison with reactions of the weakly bound ^9Be nucleus, and especially the halo nucleus ^{11}Be . Total fusion data for $^9,^{10},^{11}\text{Be}$ incident on ^{209}Bi near and below the Coulomb barrier have been obtained by Signorini *et al.* [10,11].

In the present work, elastic-scattering angular distributions for ^{10}Be incident on a ^{208}Pb target were measured at a number of energies near the barrier. The ^{10}Be beam was produced by the *TwinSol* radioactive nuclear beam facility [12]. The experimental method has previously been described [5,7]. The primary beam was ^{11}B at energies of 52–58 MeV, incident on a gas-cooled ^9Be target. (See Ref. [5] for more details concerning the target.) The secondary beam typically had an intensity of $2\text{--}3 \times 10^4$ particles per second and an energy resolution of 1.4 MeV full width at half maximum (FWHM). The secondary target was a 1.8 mg/cm² foil of isotopically separated ^{208}Pb having a purity of >99%. The experimental angular distributions are shown in Fig. 1.

The data have been analyzed in the context of the optical model. Because of the small number of data points and relatively poor statistical accuracy, extensive optical-model pa-

rameter searches were not attempted. Instead we used a simple volume Woods-Saxon form, with fixed well depths for the real and imaginary potentials. The radius and diffuseness parameters were varied to achieve good fits to the experimental angular distributions. Two different parameter sets were employed: a “shallow” real potential similar to that used by Signorini *et al.* in their analysis of the elastic scattering of ^9Be on ^{209}Bi at 42 MeV [9], and a “deep” real potential similar to that used for $^8\text{Li}+^{208}\text{Pb}$ scattering [5]. The parameters of the optical-model calculations are given in Table I, and the solid curves in Fig. 1 are the results of these calculations using the deep real potential. Also included in Table I are the computed total reaction cross sections. In general, they are similar for the two parameter sets. We used the difference between the total reaction cross sections for the two parameter sets as one measure of the experimental uncertainty. The second measure was the range of reaction cross sections within a set that results from varying the potential parameters while still achieving acceptable fits to the angular distribution. The total reaction cross sections from the optical-model fits are shown in Fig. 2, together with the

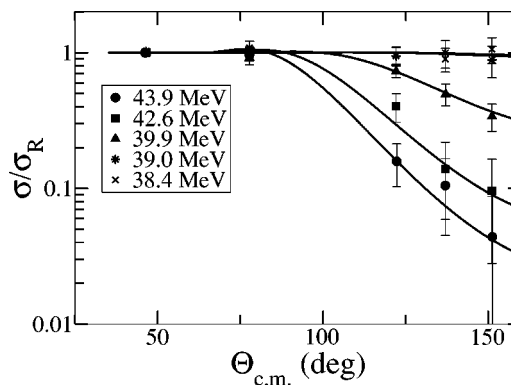


FIG. 1. Elastic-scattering angular distributions for ^{10}Be incident on ^{208}Pb . The corresponding laboratory energies are indicated. See text for a discussion of the curves.

TABLE I. Optical-model parameters and total reaction cross sections for $^{10}\text{Be}+^{208}\text{Pb}$ elastic scattering. The first set corresponds to the “shallow” real potential ($V=113$ MeV, $W=169$ MeV). The second set corresponds to the “deep” real potential ($V=270$ MeV, $W=90$ MeV). The Coulomb radius $R_C=8.95$ fm for both potentials.

$E_{c.m.}$ (MeV)	R_R (fm)	a_R (fm)	R_I (fm)	a_I (fm)	σ_r (mb)
36.6	8.59	0.63	9.66	0.30	3.0
37.2	8.59	0.63	9.66	0.30	6.0
38.1	9.43	0.63	9.66	0.50	222.0
40.6	9.43	0.63	9.66	0.50	478.0
41.9	9.43	0.63	9.66	0.50	607.0
36.6	9.48	0.38	9.92	0.35	10.0
37.2	9.48	0.38	9.92	0.39	26.0
38.1	9.48	0.55	10.25	0.42	207.0
40.6	9.48	0.54	10.31	0.43	472.0
41.9	9.48	0.52	10.82	0.46	768.0

fusion cross sections reported for $^{10}\text{Be}+^{209}\text{Bi}$ [11].

The energy dependences of the total reaction and fusion cross sections have been parametrized using the model of Wong [13] in which the complex, energy-dependent optical-model potential is replaced by an inverted harmonic oscillator potential. The reaction cross section is computed from the barrier penetration probability, leading to the formula

$$\sigma_{\text{reac}} = \left(\frac{\hbar\omega R^2}{2E_{c.m.}} \right) \ln \left[1 + \exp \left(\frac{2\pi}{\hbar\omega} [E_{c.m.} - V_b] \right) \right]. \quad (1)$$

Here, V_b is the barrier height, $\hbar\omega$ is the oscillator parameter which determines the diffuseness of the potential, and R is the radius of the system at the barrier.

The solid curve in Fig. 2 was obtained by fitting the experimental total reaction cross sections, while the dashed curve represents a fit to the $^{10}\text{Be}+^{209}\text{Bi}$ fusion data [11]. The corresponding parameters are given in Table II.

The excitation function for the total reaction cross section is consistent with $\hbar\omega=0$, i.e., the classical limit of Eq. (1).

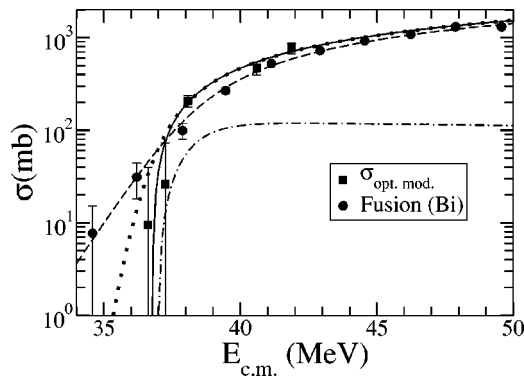


FIG. 2. Total reaction cross sections from elastic scattering of $^{10}\text{Be}+^{208}\text{Pb}$ (square points). Also shown are the fusion cross sections for $^{10}\text{Be}+^{209}\text{Bi}$ reported in Ref. [11] (circles). See text for a discussion of the curves.

TABLE II. Wong-model parameters for the total reaction and fusion cross sections of $^9,^{10}\text{Be}$ incident on high- Z targets.

System	Cross section	V_b (MeV)	R (fm)	$\hbar\omega$ (MeV)
$^{10}\text{Be}+^{208}\text{Pb}$	Total reaction	36.77	13.58	
$^{10}\text{Be}+^{209}\text{Bi}$	Fusion	37.60	13.50	6.00
$^9\text{Be}+^{209}\text{Bi}$	Total reaction	35.90	11.75	9.00
$^9\text{Be}+^{209}\text{Bi}$	Fusion	38.00	10.00	5.00

This corresponds to a barrier distribution of width zero, a behavior that is consistent with expectations for the interaction of two tightly bound nuclei.

In order to compare with the fusion data, we must first take into account the 1.7 MeV (FWHM) energy resolution of the fusion experiment [10]. The effective energy resolution of the total reaction cross section data is much better, since the experimental elastic-scattering angular distributions were obtained by comparing with the Rutherford yield averaged over the energy resolution of the beam as well as the angular resolution of the detectors. We have therefore folded these data with a Gaussian function having a width of 1.7 MeV (FWHM), and the result is shown as the dotted curve in Fig. 2. It can be seen that the total reaction cross sections are completely consistent with the fusion data, in that they equal or exceed the corresponding fusion cross sections. The difference between these two cross sections (dot-dashed curve in Fig. 2) is a measure of the “direct reaction” yield, which is seen to be small compared with the situation for, e.g., $^6\text{He}+^{209}\text{Bi}$ [1].

It is instructive to compare the reaction cross sections for ^9Be and ^{10}Be projectiles. The $^9\text{Be}+^{209}\text{Bi}$ data of Signorini *et al.* are shown in Fig. 3. The diamonds are fusion data [10,11], the square points are from a transfer/breakup measurement [11], and the stars result from an analysis of elastic scattering data [9]. (Note that the transfer/breakup yield reported in Ref. [11] has been corrected for the multiplicity of the outgoing α particles [14].) We have found that the sum of the reported fusion and transfer/breakup yields exceeds the total reaction cross section extracted from the elastic-scattering data. In order to achieve consistency with the other data sets obtained by the same group, it is necessary to multiply the measured transfer/breakup yield by a factor of 0.75.

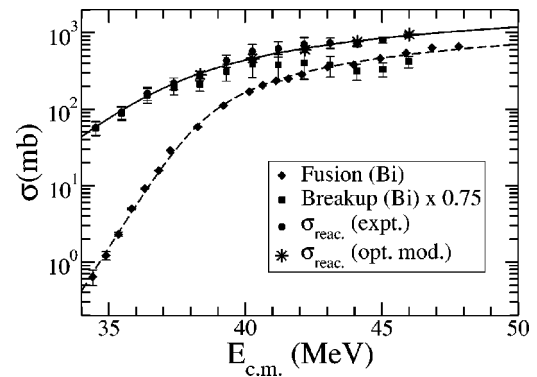


FIG. 3. Reaction cross sections for $^9\text{Be}+^{209}\text{Bi}$ measured by Signorini *et al.* See text for a discussion of these data.

The “experimental” total reaction cross sections (circular points) then agree with the optical-model result. (However, see below for a discussion of other possibilities). The solid curve through the total reaction cross section data is again a Wong-model fit, with parameters given in Table II. In comparison with the case of $^{10}\text{Be}+^{208}\text{Pb}$, it is clear that the sub-barrier yield (dominated by transfer/breakup) is very much enhanced due to the weak binding of ^9Be .

Another interesting result concerns the value of the total reaction cross section for $^{10}\text{Be}+^{208}\text{Pb}$ vs $^9\text{Be}+^{209}\text{Bi}$ at energies well above the barrier. The fusion yield for ^9Be in this “asymptotic” energy region is much smaller than that for the ^{10}Be projectile, presumably due to the large transfer/breakup cross section for ^9Be . However, the asymptotic total reaction cross section for ^9Be is also about 25% smaller than that of ^{10}Be . A very small reduction in the total reaction cross section above the barrier is to be expected [15] due to the transfer of flux into the sub-barrier regime resulting from coupling to the transfer/breakup channel, but a 25% reduction at energies well above the barrier is very surprising. The agreement would be better if the empirical reduction factor on the transfer/breakup yield discussed above were not applied, but in this case the discrepancy with the optical-model total reaction cross section is difficult to understand. Furthermore, comparison with existing fusion data [16] for $^9\text{Be}+^{208}\text{Pb}$ suggests that the $^9\text{Be}+^{209}\text{Bi}$ fusion cross section reported in Refs. [10,11] might be too large. These discrepancies suggest that further measurements of ^9Be -induced reactions are desirable.

In summary, we have measured the elastic scattering of ^{10}Be on ^{208}Pb at several energies near the Coulomb barrier.

Total reaction cross sections extracted from an optical-model analysis of the experimental angular distributions are consistent with the large fusion yield previously reported for the similar $^{10}\text{Be}+^{209}\text{Bi}$ system [10,11]. The excitation function for the total reaction cross section is consistent with penetration through a single barrier rather than a distribution of barriers, as might be expected for the interaction of two tightly bound nuclei.

Comparison with published results for $^9\text{Be}+^{209}\text{Bi}$ reveals some internal inconsistencies in these data. Specifically, the sum of the reported “fusion” and “transfer/breakup” yields exceeds the total reaction cross section deduced from an optical-model analysis of the elastic data. The discrepancy can be resolved by multiplying the reported transfer/breakup yield by a factor of 0.75, but there are other possible explanations. It also appears that the $^{10}\text{Be}+^{208}\text{Pb}$ total reaction cross section is 25% greater than that of $^9\text{Be}+^{209}\text{Bi}$ at energies well above the barrier, which is quite surprising. Further studies of ^9Be -induced reactions near the Coulomb barrier are clearly needed. However, despite these discrepancies, it seems clear that the total reaction cross section for $^9\text{Be}+^{209}\text{Bi}$ is very much enhanced compared to that of $^{10}\text{Be}+^{208}\text{Pb}$ at sub-barrier energies, due to the weakly bound nature of the ^9Be projectile.

This work was supported by the National Science Foundation under Grant Nos. PHY99-01133, PHY98-04869, PHY00-72314, and PHY98-70262, and by the CONACYT (Mexico).

[1] E. F. Aguilera *et al.*, Phys. Rev. Lett. **84**, 5058 (2000).
 [2] G. R. Kelly *et al.*, Phys. Rev. C **63**, 024601 (2001).
 [3] C. Signorini *et al.*, Eur. Phys. J. A **10**, 249 (2001).
 [4] C. Signorini *et al.*, in *Proceedings of the International Conference: Bologna 2000*, edited by G. Bonsignori, M. Bruno, A. Ventura, and D. Vretenar (World Scientific, Singapore, 2001), Vol. 1, p. 413.
 [5] J. J. Kolata *et al.*, Phys. Rev. C **65**, 054616 (2002).
 [6] C. Signorini *et al.*, Phys. Rev. C **67**, 044607 (2003).
 [7] E. F. Aguilera *et al.*, Phys. Rev. C **63**, 061603(R) (2001).

[8] N. Keeley *et al.*, Nucl. Phys. **A571**, 326 (1994).
 [9] C. Signorini *et al.*, Phys. Rev. C **61**, 061603(R) (2000).
 [10] C. Signorini *et al.*, Eur. Phys. J. A **2**, 227 (1998).
 [11] C. Signorini *et al.*, Eur. Phys. J. A **13**, 129 (2002).
 [12] M. Y. Lee *et al.*, Nucl. Instrum. Methods Phys. Res. A **422**, 536 (1999).
 [13] C. Y. Wong, Phys. Rev. Lett. **31**, 766 (1973).
 [14] C. Signorini (private communication).
 [15] S. Landowne and S. C. Pieper, Phys. Rev. C **29**, 1352 (1984).
 [16] M. DasGupta *et al.*, Phys. Rev. Lett. **82**, 1395 (1999).